Neuroradiology
https://doi.org/10.1007/s00234-021-02882-w

SHORT REPORT

Multimodal imaging of a patient with RAB39B mutation

Laurane Mackels[1] · **Martin Moïse**[2] · **Frédérique Depierreux**[3,4]

Received: 12 April 2021 / Accepted: 8 December 2021

Abstract
Mutations in *RAB39B* gene have been linked to intellectual deficiency associated with parkinsonism, also referred as to Waisman syndrome. As it appears to be a very rare cause of Parkinson Disease (PD), with only few cases described in the literature, the typical clinical and radiological features are yet to be determined. In this article, we report and illustrate multimodal brain imaging by computed tomography, magnetic resonance imaging, transcranial ultrasound (US), dopamine transporter single photon emission computed tomography and [^{18}F]-fluorodeoxyglucose positron emission tomography ([^{18}F]FDG-PET) in a 37-year-old man with PD features and mild mental retardation harboring a new *RAB39B* mutation. We then propose a comparison with data previously published regarding neuroimaging in this condition and present a summary of previous imaging reports. If our patient's results partly support previously described radiological features, they also highlight potential new characteristics of this rare syndrome. To the best of our knowledge, [^{18}F]FDG-PET and transcranial US have never been reported before in this condition. This is therefore the first multimodal brain imaging description of a patient presenting *RAB39B* mutation.

Keywords *RAB39B* · Waisman syndrome · Parkinsonism · Multimodal imaging

Case Report Our patient was born at 35 weeks of gestational age after an uncomplicated pregnancy. By the age of 11 months, axial hypotonia was noticed. Motor development and speech acquisition were delayed. Macrocephalia was documented when he was 2 years old (> 95th percentile). Autism spectrum disorder was suspected based on repetitive behaviors, overly focused interests and "body-rocking", that disappeared by the age of 5 years. In retrospect and based on the parent's descriptions, adolescence was marked by a generalised tonic-clonic seizure. During adolescence, a first brain computed tomography (CT) showed vermian hypoplasia, without basal ganglia (BG) calcification.

At the age of 37 years old, he was referred to a Movement Disorders clinic for further investigations. Clinical examination revealed parkinsonian syndrome characterized by dysarthria and dysphonia, prominent akineto-hypertonic features and rest tremor of the left hand. Mild right hemispheric cerebellar syndrome, macrocephaly, intellectual disability and frontal signs were also observed. Caryotype was normal and CGH microarray panel showed a de novo substitution mutation (c.216-2A>G) in *RAB39B* gene, consistent with our patient history and clinical features. Neuropsychological assessment slightly differed from what is typically observed in idiopathic Parkinson Disease (PD), showing alteration of short term memory, attention, verbal fluency and executive function, along with moderate ideational apraxia.

At the same age, the patient underwent a 3T brain magnetic resonance imaging (MRI). A [^{18}F]-fluorodeoxyglucose positron emission tomography ([^{18}F]FDG-PET) coupled with a low-dose CT, a dopamine transporter single photon emission computed tomography (DaT-SPECT) and a transcranial ultrasound US were acquired a few months later.

3T brain MRI protocol included axial T2-weighted turbo spin echo, axial diffusion weighted imaging (DWI), 3D FLAIR, axial, coronal and sagittal T1- weighted spin echo, both before and after intravenous injection of a gadolinium-based contrast agent, and coronal T2*-weighted

✉ Laurane Mackels

[1] Department of Neurology, CHR Citadelle of Liège, Liège, Belgium

[2] Department of Radiology, University Hospital (CHU) of Liège, Liège, Belgium

[3] Department of Neurology, University Hospital (CHU) of Liège, Liège, Belgium

[4] GIGA - CRC in Vivo Imaging, University of Liège, Liège, Belgium

Published online: 27 January 2022

gradient-echo (T2*W-GRE) sequences. It confirmed the vermian hypoplasia predominant in the inferior part. Dysgenesis of the left part of the splenium was also depicted. The body of the corpus callosum was shortened and enlarged. Measurement of cerebellar hemisphere and fourth ventricle were normal. T1W sequences showed a hypersignal in the head of caudate nucleus (CN), predominant on the right side. T2*W-GRE sequences pallidus (GP) and substantia nigra (SN) consistent with deposit of either para- or diamagnetic substances. The signal of CN was comparable to the signal of putamen (Fig. 1A–D). A few months later, in the context of parkinsonism associated with unusual cognitive defects, the patient underwent a [^{18}F]FDG-PET coupled with a low-dose CT, the latter showing marked bilateral hyperdensities in the head of CN consistent with calcifications. (Fig. 1E). We also observed much more discreet hyperdensities in GP on diagnostic displays, raising suspicion for calcifications in this area as well (see supplementary data).

[^{18}F]FDG-PET showed a cortical hypofixation in the frontal and supra-orbital areas, more prominent on the left side. A symmetric temporal hypofixation was also noticed, along with a discrete hypofixation in the thalami and left striatum. (Fig. 1F). Signal was symmetric in both cerebellar hemispheres.

DaT-SPECT and transcranial US were acquired shortly after [^{18}F]FDG-PET and CT. DaT-SPECT showed reduced activity in posterior putamen bilaterally, consistent with a severe dysfunction of presynaptic dopaminergic pathways (Fig.1I). Transcranial US of the midbrain using temporal bone window revealed that the area of hyperechogenicity at the anatomical site of the SN was significantly enlarged, particularly on the right side (Fig. 1G).

Discussion

PD is a frequent neurodegenerative disorder, typically occurring at an average age of 60 years, and causing four cardinal motor signs (resting tremor, rigidity, bradykinesia and postural instability) along with non-motor symptoms (hyposmia, rapid eye movement (REM) sleep behavioural disorders (RBD), etc.). Although PD is mainly idiopathic, approximately 5–10% of cases are due to known monogenic mutations. *RAB39B* is one of the rare recessive X-linked Mendelian PD genes that have been identified so far [1, 2]. *RAB39B* is located on the Xq28 chromosome and encodes for a neuron specific RAB GTPase that plays an important role on vesicle trafficking and secretory pathways in neuronal cells [1, 3–7].

RAB39B pathogenic variants were first identified in 2010 by Giannandrea et al. in patients presenting X-linked Intellectual Disability (XLID) with autism spectrum disorder, macrocephaly and epilepsy [8]. In 2014, Wilson et al. identified two novel mutations in two unrelated families displaying early-onset parkinsonism and variable degrees of intellectual disability, also referred to as Waisman syndrome [5]. Overall, the broad clinical spectrum reported in the literature includes childhood-onset intellectual disability, young-onset Parkinsonism with partial or good levodopa response, spastic paraparesis, cerebellar dysfunction, dysarthria, macroencephaly and epilepsy [3, 6, 7]. Parkinsonian signs seem more likely to appear after the second decade, although found earlier in few patients [4, 5]. Clinical characteristics of our patient overlap those previously reported features. Mild cerebellar dysfunction was described in only one other patient carrying *RAB39B* mutation [5] and may be a part of the neurological phenotype of the disease.

Post-mortem histological studies demonstrated that loss of *RAB39B* resulted in dopaminergic neuronal loss and extracellular iron deposits in the SN, along with other characteristics consistent with pathologically confirmed PD [3, 5]. Regarding radiological features, some authors have described iron accumulation in the BG and SN [3, 5, 6] while others have reported calcification in BG [3, 4].

As stated above, brain CT might display high-density calcifications in GP and SN. However, it remains an inconstant feature that has not been confirmed in all post-mortem or imaging studies [3, 5] (Table 1). Regarding our patient, calcification of BG were not found on the first CT but were depicted later in life, at the age of 37 years old.

Reproducible MRI findings throughout literature included T1W, T2W, T2*W-GRE and susceptibility weighted imaging SWI low signal in GP and SN [3, 4, 6]. More subtle hypointensities in SWI sequences were also described in red nucleus (RN), putamen and pulvinar. [3] (Table 1). For some authors, these hyposignals in T2*W-GRE sequences are thought to represent iron deposition [3, 6]. As for our patient, MRI depicted T2*W-GRE hyposignals in both GP and SN, while CT showed calcification in the head of CN but not in the SN. We also observed very discreet, yet suspicious hypersignals in GP. Given the clinical context of parkinsonism, the T2*W-GRE hypointensities might be due to iron deposition, although calcification could also be present. Interestingly, iron accumulation in BG and particularly in SN is also a typical feature of classical PD [9] and would therefore be expected to be found in these particular areas in the setting of RAB39b mutations. More data are needed in order to clarify the pathology of this condition regarding calcium versus iron deposits. In this regard, SWI-filtered phase images analysis would be of great diagnostic interest in differentiating between diamagnetic and paramagnetic susceptibility effects of calcium and iron, respectively. In this case, MRI also displayed inferior vermian hypoplasia along with shortened corpus callosum and dysgenesis of the left side of the splenium. Those features have not been described yet

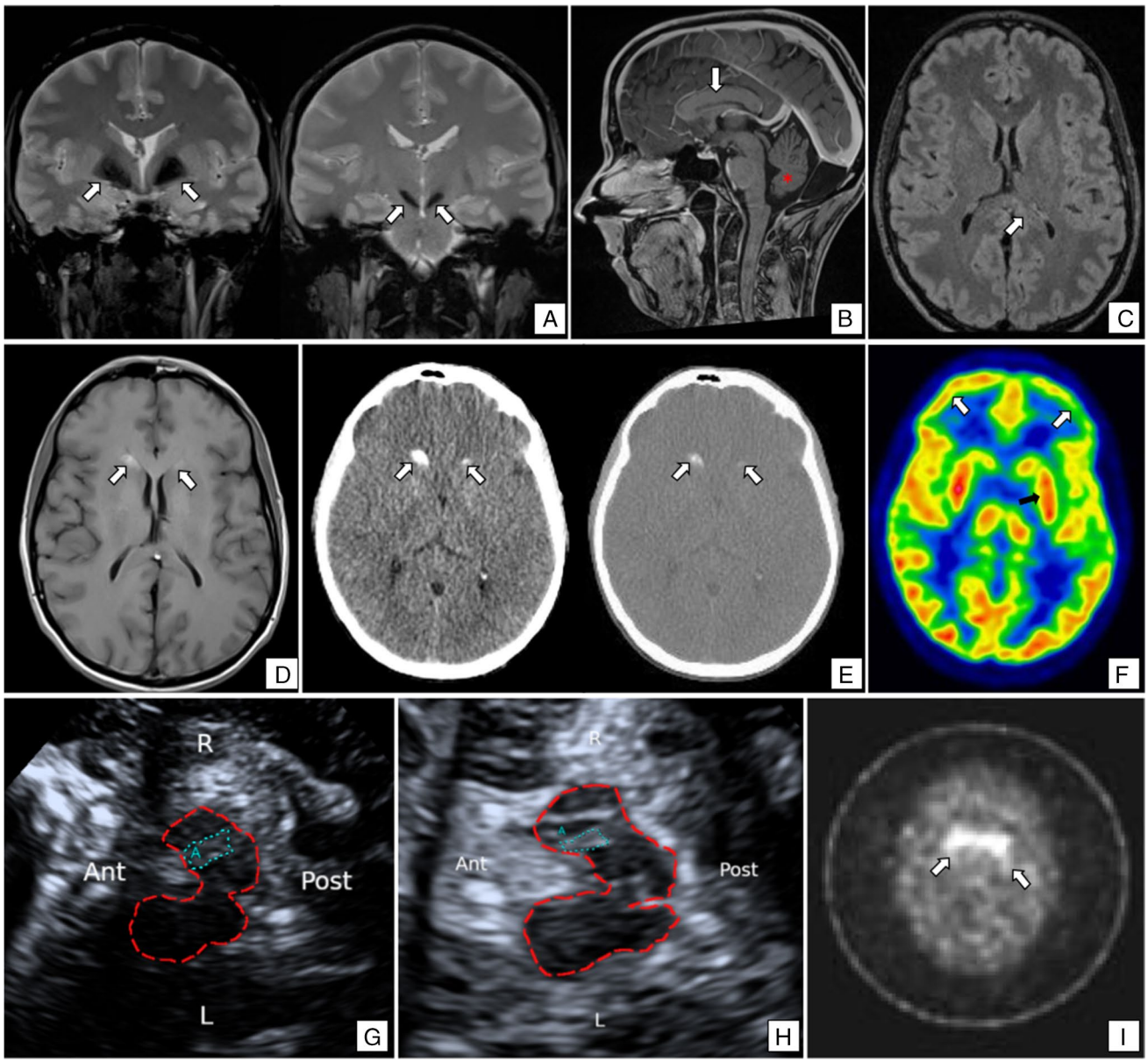

Fig. 1 A) Coronal sections in T2*W-GRE showing hyposignals in GP and SN, consistent with deposit of paramagnetic substances in this area (white arrows). B) Sagittal T1W showing hypoplasia of the inferior part of the vermis with an enlargement of the cisterna magna (red star), along with a shortened and thickened corpus callosum (white arrow). C) Axial FLAIR section showing dysgenesis of the left side of the splenium. D) Axial T1W showing an hypersignal in the head of CN predominant on the right side, due to shortened T1 around microcalcifications (white arrows). E) Brain (left) and bone (right) windows of low-dose head CT showing bilateral calcification in CN (white arrows). Very subtle calcifications were hardly noticed in GP on diagnostic displays. They are not illustrated because of insufficient resolution of these pictures for publication but they might be better depicted on the picture available in the supplementary data. F) [^{18}F]FDG-PET displaying a bilateral and slightly asymmetric cortical hypofixation in the frontal and supra-orbital area, more pronounced on the left side (white arrows). Other features include symmetric temporal hypofixation, discret hypofixation in the thalami and the left striatum (black arrow). G) Transcranial US showing enlarged area of hyperechogenicity (area: 0,65 cm^2) (blue dots) at the anatomical site of the right sn in the mesencephalon (red dots), when compared to H) a control subject (area: 0,15 cm^2). I) Transverse planes of DaT-SPECT showing bilateral reduced activity in posterior putamen (white arrows)

in *RAB39B*-related PD and may represent novel radiological characteristics of this syndrome.

DaT-SPECT and ^{123}I-iodobenzamide (IBZM)-single photon emission computed tomography (SPECT) performed in very few patients were consistent with pre- and postsynaptic nigrostriatal dopaminergic degeneration (Table 1). Our results support these data, showing reduced activity in posterior putamen bilaterally, compatible with a severe

Table 1 Summary of imaging reports in patient with *RAB39B* mutation

Authors	Mutation	Sex	Parkinsonism (age at onset)	CT	MRI	Functional Imaging
Lesage et al. [1]	Nonsense mutation c.557G. Ain exon 2 [p.Trp186stop]	M	39y	N/A	Normal	N/A
Ciammola et al. [3]	Frameshift variant c.137dupT	M	11y	Moderate GP calcification	fat spin echo (FSE) T2 and T2*W-GRE hypointensities in GP and SN. Lighter hypointensities in RN, putamen and pulvinar bilaterally	DaT-SPECT: severe reduction of radioligand uptake at left putaminal nucleus
	Frameshift variant c.137dupT	M	60y	Bilateral GP calcification	N/A	N/A
	Deletion variant c.371delA	M	44y	No calcification	SWI and T2*W-GRE strong hypointensity signal in SN and GP. Less intensive in RN, putamen and pulvinar	DaT-SPECT: moderate symmetrical reduction of radioligand uptake at putaminal nuclei and slight reduction at CN
Shi et al. [4]	Frameshift mutation c. 536dupA (p.E179fsX48)	M	10y	Bilateral GP calcification	T1, T2 and SWI low signal intensities in the bilateral GP	N/A
		M	12y	Bilateral GP calcification	T1, T2 and SWI low signal intensities in the bilateral GP	N/A
Wilson et al. [5]	All gene deletion 45kb	M	Childhood	N/A	N/A	N/A
		M	38y	N/A	Normal	N/A
		M	44y	N/A	T2 slight bilateral reduction in signal intensity in SN and GP	N/A
	Point mutation c.503C>A [p.Thr168Lys]	13M and 1F	10-20's	Megalencephaly	N/A	N/A
Güldner et al. [6]	Hemizygous single base pair deletion c.432delA	M	29y	N/A	T2*W-GRE hypointensities in BG and SN.	DaT-SPECT and IBZM-SPECT : Pre- and postsynaptic dopaminergic deficits
Mata et al. [7]	Missense mutation (c.574G > A; p.G192R	5M	29y – 31y – 48y – 50y – 53y	N/A	N/A	N/A
		2F	55y – 57y	N/A	N/A	N/A

dysfunction of presynaptic dopaminergic pathways. To our knowledge, [^{18}F]FDG-PET has never been reported before in this condition. Our patient's [^{18}F]FDG-PET showed a left-predominant cortical hypofixation in the frontal and supra-orbital area along with a symmetric temporal hypofixation and a discrete hypofixation in the thalami and left striatum.

We performed the first transcranial US in a *RAB39B* patient using temporal bone window. It displayed bilateral and slighly asymmetric hyper-echogenic signals in the mid-brain and more specifically in the SN. Such features have been previously described in PD patients as the result of higher tissue iron level in these particular areas [10]. In our case, the enlarged area of hyperechogenicity at the anatomical site of the SN may indicate iron accumulation, which is consistent with the strong reduction in T2*W-GRE signal intensity and corroborates the pathological findings of previous postmortem and radiological studies [3, 5].

Conclusion

This case report supports previous findings (Table 1) and highlights potential novel neuroimaging features related to *RAB39B* mutation. Idiopathic PD is typically characterized by normal routine MRI and [^{18}F]FDG-PET pattern. Therefore, the presence of corpus callosum abnormality or cerebellar involvement in routine MRI and atypical [^{18}F]FDG-PET pattern in a patient suspected to present early-onset or juvenile PD should raise the attention of both radiologist and clinician, eventually leading to appropriate genetic testing. More data are needed in order to clarify the pathology of this condition regarding the deposition of calcium versus iron in BG and SN. In this respect, SWI-filtered phase images analysis would be of great diagnostic interest in differentiating between diamagnetic and paramagnetic susceptibility effects of calcium and iron, respectively. The interpretation of our patient's US and MRI suggests iron accumulation in SN. We also observed that calcification in BG were initially absent and appeared later on, during adulthood. As the appearance of calcifications on CT in the BG is variable and may be absent early in the patient life, their absence should not exclude the diagnosis.

Supplementary Information The online version contains supplementary material available at https://doi.org/10.1007/s00234-021-02882-w.

Author Contributions The three authors made substantial contributions to the manuscript. Laurane Mackels was responsible for the data analysis, literature review, and writing of the manuscript. Martin Moïse reviewed the different versions of the manuscript. Frédérique Depierreux collected the clinical data and reviewed the different versions of the manuscript. The three authors read and approved the final version of the article prior to submission.

Funding No funding was received for this report.

Declarations

Conflicts of interest The authors declare that they have no conflict of interest.

Ethical approval This work raises no ethical concerns.

Informed consent Informed consent was obtained from the patient for this case report.

References

1. Lesage S, Bras J, Cormier-Dequaire F, Condroyer C, Nicolas A, Darwent L, Guerreiro R, Majounie E, Federoff M, Heutink P, et al (2015) Loss-of-function mutations in rab39b are associated with typical early-onset parkinson disease. Neurol Genet 1(1) https://doi.org/10.1212/NXG.0000000000000009
2. Gao Y, Wilson GR, Salce N, Romano A, Mellick GD, Stephenson SE, Lockhart PJ (2020) Genetic analysis of rab39b in an early-onset parkinson's disease cohort. Front Neurol 11 https://doi.org/10.3389/fneur.2020.00523
3. Ciammola A, Carrera P, Di Fonzo A, Sassone J, Villa R, Poletti B, Ferrari M, Girotti F, Monfrini E, Buongarzone G et al (2017) X-linked parkinsonism with intellectual disability caused by novel mutations and somatic mosaicism in rab39b gene. Parkinsonism & Related Disorders 44:142–146. https://doi.org/10.1016/j.parkreldis.2017.08.021
4. Shi CH, Zhang SY, Yang ZH, Yang J, Shang DD, Mao CY, Liu H, Hm Hou, Shi MM, Wu J et al (2016) A novel rab39b gene mutation in x-linked juvenile parkinsonism with basal ganglia calcification. Movement Disorders 31(12):1905–1909. https://doi.org/10.1002/mds.26828
5. Wilson GR, Sim JC, McLean C, Giannandrea M, Galea CA, Riseley JR, Stephenson SE, Fitzpatrick E, Haas SA, Pope K et al (2014) Mutations in rab39b cause x-linked intellectual disability and early-onset parkinson disease with α-synuclein pathology. The American Journal of Human Genetics 95(6):729–735. https://doi.org/10.1016/j.ajhg.2014.10.015
6. Güldner M, Schulte C, Hauser AK, Gasser T, Brockmann K (2016) Broad clinical phenotype in parkinsonism associated with a base pair deletion in rab39b and additional polg variant. Parkinsonism & Related Disorders 31:148–150. https://doi.org/10.1016/j.parkreldis.2016.07.005
7. Mata IF, Jang Y, Kim CH, Hanna DS, Dorschner MO, Samii A, Agarwal P, Roberts JW, Klepitskaya O, Shprecher DR et al (2015) The rab39b p. g192r mutation causes x-linked dominant parkinson's disease. Molecular neurodegeneration 10(1):1–8. https://doi.org/10.1186/s13024-015-0045-4
8. Giannandrea M, Bianchi V, Mignogna ML, Sirri A, Carrabino S, D'Elia E, Vecellio M, Russo S, Cogliati F, Larizza L et al (2010) Mutations in the small gtpase gene rab39b are responsible for x-linked mental retardation associated with autism, epilepsy, and macrocephaly. The American Journal of Human Genetics 86(2):185–195. https://doi.org/10.1016/j.ajhg.2010.01.011
9. Pyatigorskaya N, Morere CBS, Gaurav R, Valabregue R, Santin MD, Yahia Cherif L, Lehéricy S et al (2020) Iron imaging as a diagnostic tool for parkinson's disease: A systematic review and meta-analysis. Frontiers in Neurology 11:366. https://doi.org/10.3389/fneur.2020.00366
10. Berg D (2006) In vivo detection of iron and neuromelanin by transcranial sonography-a new approach for early detection of substantia nigra damage. Journal of Neural Transmission 113(6):775–780. https://doi.org/10.1007/s00702-005-0447-5

Terms and Conditions

Springer Nature journal content, brought to you courtesy of Springer Nature Customer Service Center GmbH (“Springer Nature”).
Springer Nature supports a reasonable amount of sharing of research papers by authors, subscribers and authorised users (“Users”), for small-scale personal, non-commercial use provided that all copyright, trade and service marks and other proprietary notices are maintained. By accessing, sharing, receiving or otherwise using the Springer Nature journal content you agree to these terms of use (“Terms”). For these purposes, Springer Nature considers academic use (by researchers and students) to be non-commercial.
These Terms are supplementary and will apply in addition to any applicable website terms and conditions, a relevant site licence or a personal subscription. These Terms will prevail over any conflict or ambiguity with regards to the relevant terms, a site licence or a personal subscription (to the extent of the conflict or ambiguity only). For Creative Commons-licensed articles, the terms of the Creative Commons license used will apply.
We collect and use personal data to provide access to the Springer Nature journal content. We may also use these personal data internally within ResearchGate and Springer Nature and as agreed share it, in an anonymised way, for purposes of tracking, analysis and reporting. We will not otherwise disclose your personal data outside the ResearchGate or the Springer Nature group of companies unless we have your permission as detailed in the Privacy Policy.
While Users may use the Springer Nature journal content for small scale, personal non-commercial use, it is important to note that Users may not:

1. use such content for the purpose of providing other users with access on a regular or large scale basis or as a means to circumvent access control;
2. use such content where to do so would be considered a criminal or statutory offence in any jurisdiction, or gives rise to civil liability, or is otherwise unlawful;
3. falsely or misleadingly imply or suggest endorsement, approval , sponsorship, or association unless explicitly agreed to by Springer Nature in writing;
4. use bots or other automated methods to access the content or redirect messages
5. override any security feature or exclusionary protocol; or
6. share the content in order to create substitute for Springer Nature products or services or a systematic database of Springer Nature journal content.

In line with the restriction against commercial use, Springer Nature does not permit the creation of a product or service that creates revenue, royalties, rent or income from our content or its inclusion as part of a paid for service or for other commercial gain. Springer Nature journal content cannot be used for inter-library loans and librarians may not upload Springer Nature journal content on a large scale into their, or any other, institutional repository.
These terms of use are reviewed regularly and may be amended at any time. Springer Nature is not obligated to publish any information or content on this website and may remove it or features or functionality at our sole discretion, at any time with or without notice. Springer Nature may revoke this licence to you at any time and remove access to any copies of the Springer Nature journal content which have been saved.
To the fullest extent permitted by law, Springer Nature makes no warranties, representations or guarantees to Users, either express or implied with respect to the Springer nature journal content and all parties disclaim and waive any implied warranties or warranties imposed by law, including merchantability or fitness for any particular purpose.
Please note that these rights do not automatically extend to content, data or other material published by Springer Nature that may be licensed from third parties.
If you would like to use or distribute our Springer Nature journal content to a wider audience or on a regular basis or in any other manner not expressly permitted by these Terms, please contact Springer Nature at

onlineservice@springernature.com